METAL PORPHYRIN COMPLEXES WITH NOVEL FUNCTIONS

Zen-ichi Yoshida

Department of Synthetic Chemistry, Kyoto University, Yoshida, Kyoto 606, Japan

Abstract —— Porphyrins reveal novel functions by metal complex formation. In this lecture following work in our laboratories is described: (1) oxygen binding and activation function of heme (porphyrin Fe(II) complex), (2) monooxygenation function of porphyrin oxovanadium complex (cytochrome P-450 mimic), and (3) catalytic function of porphyrin cobalt complex for valence isomerization (quadricyclanes to norbornadienes).

Introduction

So far organic chemistry, particularly organic synthesis has been directed toward "structure synthesis" where structure-determined compounds (eg. natural products) or structure-designed new systems (eg. planar $4n\pi$ ring systems, highly strained ring systems) have been the synthetic target. On the other hand, "function synthesis" (or "function chemistry") is recently being given attention as a new field in organic chemistry. The function synthesis should be achieved by repeating the following three steps: (1) molecular elucidation of target function, (2) molecular design based on this results, and (3) synthetic approach to the designed molecule. As such examples, I would like to describe here transition metal porphyrin complexes with novel functions whose chemistry has been developing in our laboratories.

1. Reversible Oxygen Binding and Oxygen Activation with Heme

Heme is known to be the active site of hemoproteins, which exhibit the different biological function such as (1) reversible oxygen binding for transport and storage (hemoglobin and myoglobin), and (2) oxygen activation (monooxygenase such as cytochrome P-450, and dioxygenase such as L-tryptophan pyrrolase). (see Fig. 1) The most significant problem in both cases is why same heme (protoheme) of their active site can stabilize molecular oxygen as is seen in myoglobin (Mb) and hemoglobin (Hb) on the one hand, and can activate molecular oxygen as is seen in tryptophan pyrrolase (TPO) and cytochrome P-450 on the other hand. To elucidate this problem, (1) the reversible oxygen binding using the reconstituted Mb and the bridged heme, and (2) oxygen activation in TPO using the synthetic heme as a model

of its active site have been investigated. We synthesized various hemins (Table 1) and recombined them with sperm whale apo-Mb to get reconstituted met Mb (r-met Mb). After

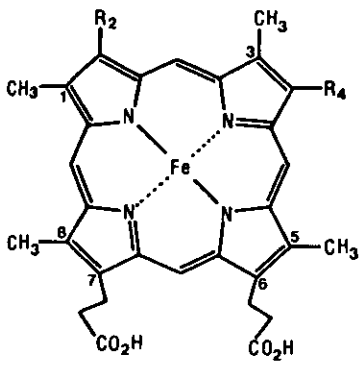

Heme used

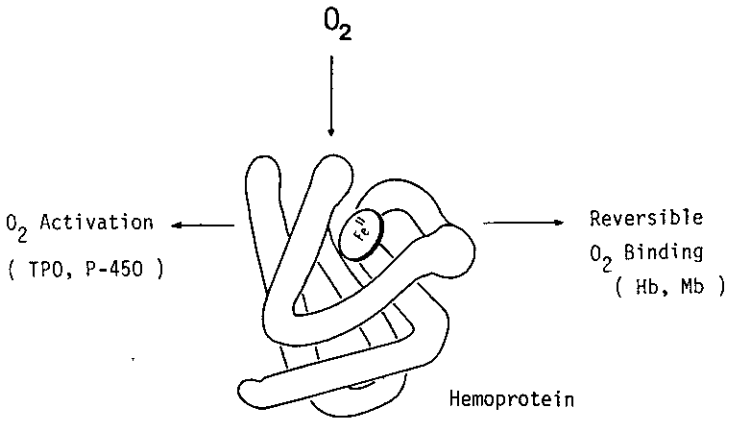

Fig. 1 Schematic views of reversible O_2 binding and O_2 activation with hemoprotein

Table 1 Oxygen affinity (P_{50} at pH 7.4, 25°C) and pKa (25°C) of Reconstituted Sperm Whale Myoglobin

Heme	R_2	R_4	P_{50} (mmHg)	pKa
proto-	$-CH=CH_2$	$-CH=CH_2$	0.91	8.95
pempto-	-H	$-CH=CH_2$	0.68	8.90
isopempto-	$-CH=CH_2$	-H	0.49	9.00
deutero-	-H	-H	0.33	9.10
2-Et,4-H-	$-CH_2CH_3$	-H	0.40	9.32
meso-	$-CH_2CH_3$	$-CH_2CH_3$	0.66	9.4
2-Ip,4-V-	$-CH(CH_3)_2$	$-CH=CH_2$	0.56	
2-V,4-Ip-	$-CH=CH_2$	$-CH(CH_3)_2$	2.46	
DIP-	$-CH(CH_3)_2$	$-CH(CH_3)_2$	3.98	9.50
DNPe-	$-CH=CHCH_3$	$-CH=CHCH_3$	1.15	9.06
DIBe-	$-CH=C(CH_3)_2$	$-CH=C(CH_3)_2$	0.19	
DIB-	$-CH_2CH(CH_3)_2$	$-CH_2CH(CH_3)_2$	0.26	
DNBy-	$-CO(CH_2)_2CH_3$	$-CO(CH_2)_2CH_3$	7.60	
DNVe-	$-CH=CH(CH_2)_2CH_3$	$-CH=CH(CH_2)_2CH_3$	1.59	
DNVy-	$-CO(CH_2)_3CH_3$	$-CO(CH_2)_3CH_3$	7.00	

reduction of the r-met Mb to the corresponding reconstituted Mb (r-Mb), the value of oxygen pressure at half saturation, P_{50} (measure for oxygen affinity) was determined. The value of oxygen affinity is summarized in Table 1 together with the pKa value (a measure of relative electron density of heme iron) of the H_2O-coordinated met Mb.[1]

Table 1 shows that the effect of the substituents (R_2, R_4) on oxygen affinity of r-Mb cannot be explained consistently by either the electronic effect or the bulkiness effect of R_2 and R_4, although both effects are important. To explain consistently the altered oxygen affinities for r-Mb, it is required to consider the stereochemical interaction between the heme and the heme-contact protein residues in heme pocket upon oxygenation. This is because of the change of stereostructure of proximal histidine-coordinated heme (pentacoordinated complex) to the near planar structure by heme movement before the formation of oxygenated heme (hexa-coordinated complex). Detailed discussion on this subject is not the purpose of this lecture and it has been made elsewhere.[1,2] So I would like to emphasize here that the existence of proximal histidine (F8)-coordinated heme in the heme pocket is very important for reversible oxygen binding of r-Mb. (see Fig. 2)

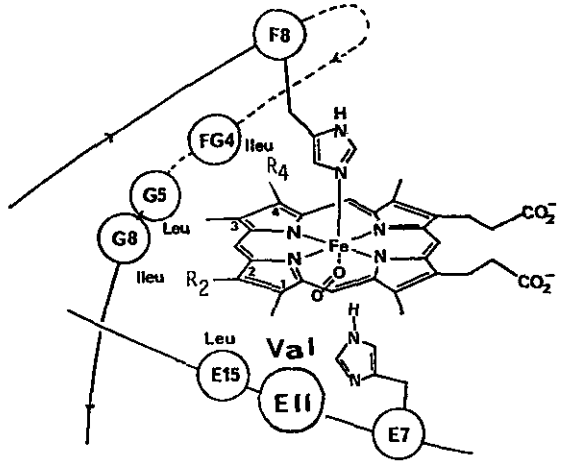

Fig. 2 Oxygen binding structure around the heme in Mb

In order to examine the effect of hydrophobic cavity size in heme pocket on the stability of r-Mb·Fe(II)O_2, we have synthesized the bridged porphyrins and prepared their iron and cobalt complexes (1).[2,3] The stability of the oxy form of the bridged iron(II)porphyrin (n=6 ∿ 14) in the following solvent-reducing agent systems is determined by spectroscopic method:

solvent system A: Toluene-N-ethylimidazole with $NaBH_4$

solvent system B: DMF-N-ethylimidazole with $NaBH_4$

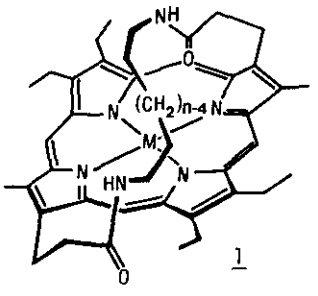

1

[n]-Bridged Metalloporphyrin M: Fe, Co, n: 6∿14

The observed half life time of the oxy form in each solvent system at 233°K and 273°K is summarized in Table 2. The stability of [n]-hydrocarbon chain-bridged iron(II) porphyrin · (N-ethylimidazzole) · O_2 is clearly shown to become large with decreasing cavity size until n=6. The CPK model for the oxygen adduct indicates that the bound oxygen best fits for the cavity of the [6] bridged one.

Table 2 Half Life Time (min) of Bridged Iron(II)porphyrin·(N-Ethylimidazole)·O_2

Solvent system	233°K		273°K	
	A	B	A	B
n=6	110	170	8	15
8	70	160	5	15
10	60	100	5	14
12	60	110	5	13
14	60	110	5	13
ref.*1	45	55	0.5	1.5

*1) reference compound: non-bridged system

Although it is not able to obtain the oxy form of the bridged heme (I, M: Fe(II)) at room temperature, the [n]-bridged Co(II)porphyrin 1, M: Co(II), n: 7, 10, 12, 14) is found to form the reversible oxygen binding adduct at ambient temperature (eg. 25°C). For example, the reversible oxygen binding with [12] bridged Co(II)porphyrin in DMF-benzimidazole is illustrated in Fig. 3. The absorption spectra (399, 550 nm) observed in the absence of oxygen

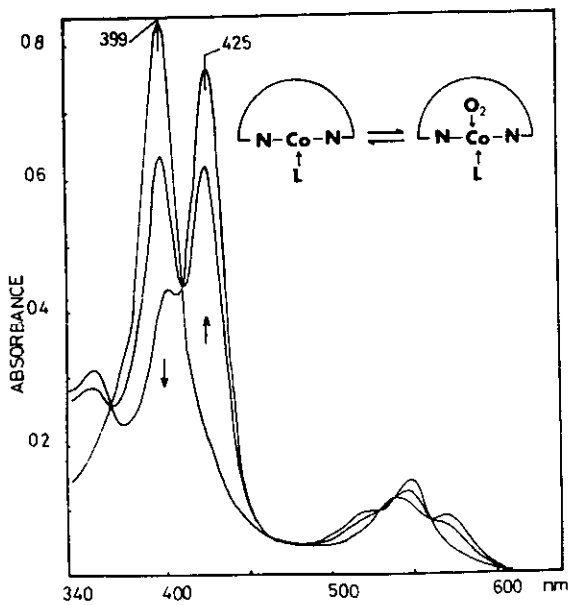

Fig. 3 Absorption spectra of reversible oxygenation of [12] bridged Co(II)porphyrin in DMF-benzimidazole (L), 25°C

are a typical pattern of the deoxyform (the five coordinated monoamine adduct). On the other hand, the absorption spectra (425, 540, 565 nm) observed in the presence of oxygen indicate the formation of the 1:1 stoichiometric complex, [12] bridged Co(II)porphyrin·(benzimidazole)·O_2. N-ethylimidazole behaves similar to benzimidazole. So it is concluded that imidazole nitrogen ($\gg$N) is very important for the formation of reversible oxygen adduct (Im-Fe(II)P-O_2) in the bridged metalloporphyrin as well as in the reconstituted Mb. Then I would like to discuss the activation of molecular oxygen in tryptophan pyrrolase (TPO) using the model.

TPO catalyses the reaction of tryptophan (R: $CH_2CH(NH_2)CO_2H$) with molecular oxygen to

form formylkynurenine (FK) according to equation 1.

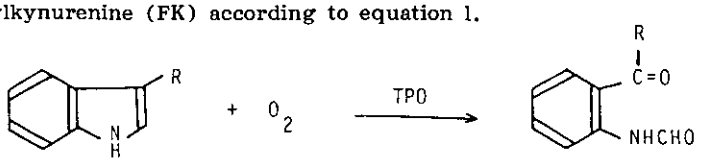

(1)

The most remarkable feature of this enzyme reaction system is that the presence of a reductase system is not required. Detailed analysis of the TPO reaction indicates that the reduced TPO (Fe(II)TPO) is the active form of this enzyme and that TPO has two kinds of binding sites which form the substrate-enzyme adduct ($EFe^{2+}\cdot S_1S_2$) with tryptophan. This adduct's interaction with molecular oxygen yields the oxygenated adduct ($EFe^{2+}\cdot S_1S_2\ O_2$), which decomposes to FK and $EFe^{2+}\cdot S_1$. (see Fig. 4). The electronic spectra of Fe(II)TPO,

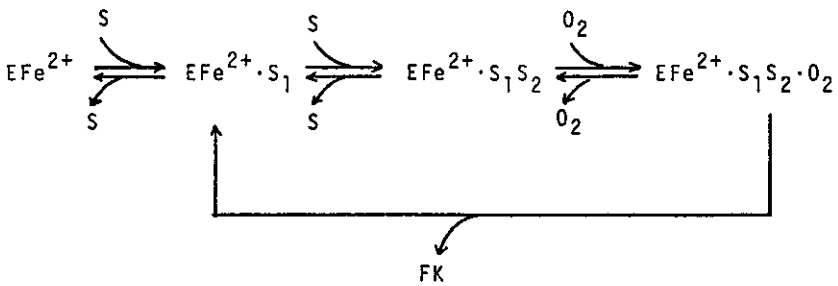

Fig. 4 TPO reaction cycles

Fe(III)TPO, and Fe(II)TPO O_2 are very similar to those of myoglobin.[4,5] Based on the spectral similarity between myoglobin and TPO, we deduced that the surrounding structure of the heme in TPO is similar to that in myoglobin. With this in mind, we chose the iron(II) complexes of octaethylporphyrin and tetraphenylporphyrin, (OEP·Fe(II)py_2 and TPP·Fe(II)py_2, respectively, as models of the TPO active site and benzene as the hydrophobic environment surrounding the heme and carried out the following model reactions. Skatole (2 mmol R: CH_3 in eq. 2) in benzene (10 ml) is difficult to react with oxygen (1 atmosphere) at room temperature (23° ± 2°C). However, in the presence of TPP·Fe(II)py_2 or OEP·Fe(II)py_2 (20 μ mol, substrate/TPO model molar ratio: 100/1) oxygen absorption easily occurs and skatole is converted to 2-formamidoacetophenone (FA, R: CH_3 in eq. 2) as shown in equation 2.

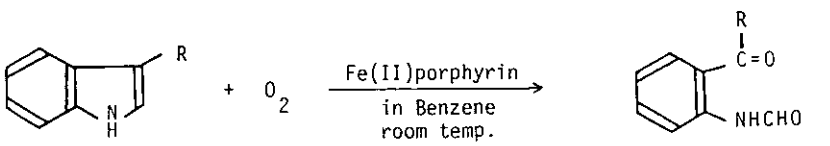

(2)

The conversion of skatole increases with time (Fig. 3). At less than 40∿50% conversion, FA is the sole product. On the other hand, at over 50% conversion, products other than FA are formed and the amount of byproducts formed increases with time. For example, at 90% conversion of skatole, the yield of FA is 44% and the remainder (56%) of the skatole becomes 2-aminoacetophenone and polymeric materials. Both porphyrins (TPP·Fe(II)·py_2 and OEP·Fe(II)·py_2) show almost the same catalytic activity for this reaction. When N-ethylimidazole is added to this reaction system, the reaction of skatole with oxygen is depressed with the amount of N-ethylimidazole added (Fig. 4). This is ascribed to the masking effect of the active

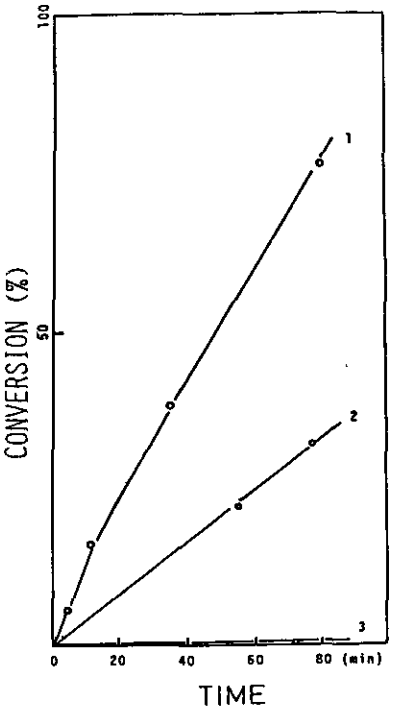

1. Skatole
2. Skatole (Skatole: N-ethylimidazole = 1 : 0.23) (molar ratio)
3. Skatole (Skatole: N-ethylimidazole = 1 : 5.5) (molar ratio)

Fig. 5 Oxygenation reaction of skatole

coordination site by the stronger ligand, indicating the importance of the coordination of skatole to Fe(II) porphyrin. The spectroscopic monitoring of the reaction mixture indicates that the μ oxodimer (TPP·Fe(III)OFe(III)·TPP) is slowly formed by the oxidation of TPP·Fe(II) complex. However it was found that (1) the catalytic activity of the μ-oxo dimer for this oxygenation is low compared to that of TPP·Fe(II)py_2, and (2) the μ-oxo dimer and TPP·Fe(III)X are almost inactive catalyst for the oxygenation of 3-t-butylindole, which is easily oxygenated by TPP Fe(II)py_2 to form the same type product as FA. Although tryptophan does not dissolves in

benzene, 3-indolepropionic acid ester (R' = CH_3 C_6H_{13}) is soluble in benzene, and converted smoothly to the corresponding 2'-formamidophenyl-4-ketopropionic ester (see eq. 3). The

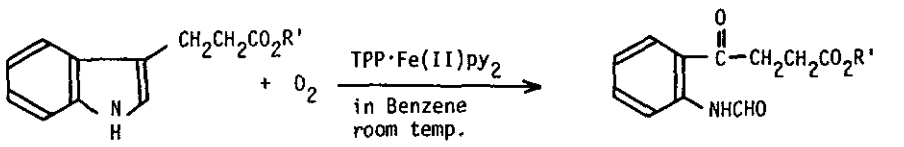

(3)

reaction proceeds more effectively with increasing alkyl chain length (R'). Therefore, judging from the oxygenation activity, the high product selectivity, the high product yield, and the structural similarity to TPO active site, the iron(II)porphyrin system is considered to be the best model of TPO active site. As for the substrate specificity of rion(II)porphyrin catalyzed oxygenation, 3-alkyl and 2,3-dialkylindoles undergo the TPO type reaction. However, indole, 2-methylindole, 1,2-dimethylindole, and 1,3-dimethylindole do not react with oxygen under the above conditions. For indole derivatives to be oxygenated catalytically by Fe(II)porphyrin (heme), they must have a 3-alkyl group and a N-H group. This substrate specificity is different than those in photosensitized oxygenation by singlet oxygen and radical autoxidation of indole derivatives, suggesting that the active oxygen species produced from 3-alkylindole-Fe(II)porphyrin-O_2 system is different than the singlet oxygen and radical oxygen species from autoxidation. Although oxygen coordinates to the Fe(II) of iron-porphyrin in aprotic solvents, the electronic and NMR spectra of the skatole-Fe(II)TPP and skatoleFe(III)TPP systems indicate the σ coordination (2) of skatole NH toward iron is difficult to accomplish. Therefore, the π interaction of skatole with the iron of Fe(II)TPP·O_2 and the σ-coordination of skatole N^- (produced through deprotonation by iron porphyrin) with the iron of Fe(II)·TPP complex should occur for the skatole → FA reaction; the equilibrium concentration of this complex should be small. However the substrate specificity mentioned above excludes the possiblity of oxygen activation via the π coordinated skatole Fe(II)porphyrin-O_2 complex (3). So the oxygen activation in this reaction system seems to occur via a skatole anion-coordinated Fe(II)porphyrin-O_2 complex (4).

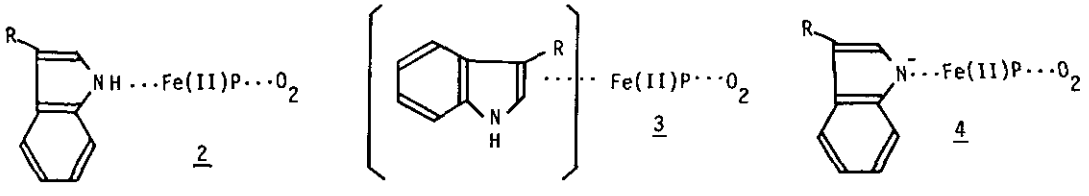

To gain insight into the oxygen activation mechanism of this model system ESR investigation of the following systems was carried out in toluene: 1. TPP·Fe(II)·py_2 (10 μ mol)-skatol (1 mmol); 2. TPP·Fe(II)py_2-skatole-air; 3. TPP·Fe(III)·OAc-skatole; and 4. Skatole-air system. Using air instead of oxygen, we can control the reaction rate to get the ESR spectra for systems 1-4 at different times. The ESR measurement was carried out at -196°C (liq. N_2 temperature) after allowing the solution to stand at 23°C ± 2° for a given period of time. For systems 1,3, and 4 no ESR signal was detected for one day immediately after preparation. In the absence of molecular oxygen electron transfer does not occur between skatole (or skatole anion) and the Fe(III)porphyrin. Immediately upon contact with air, the high spin complex due to Fe(III)TPPpy was observed together with the free radicals whose g values are 1.99 - 2.04 and the low spin Fe(III) complex. The appearance of ESR absorptions due to Fe(III) complexes (high and low spin) indicates that a part of Fe(II)TPP complex is converted to the Fe(III) state by reaction with molecular oxygen. The absorption at g = 1.99 is assigned to the superoxide ion ($\cdot O_2^-$ coordinated to the heme iron). There is a very broad band centered at g = 2.04 that has hyperfine splittings. The each hyperfine constant is very large (ca. 20G) compared with those for the pyrryl π radicals (6) Therefore, this radical can be identified as the following skatole σ radical (5). The σ radical (5) and iron-coordinated superoxide ion ($\cdot O_2^-$) are

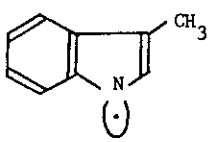

5

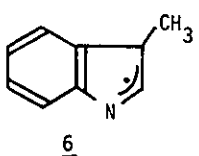

6

considered to be formed by electron transfer from the skatole anion to oxygen in the ternary complex (4), which is composed of strong electron donor and weak electron acceptor through Fe(II)porphyrin. In such a complex (D····Fe(II)P····A type complex, D: electron donor, A: acceptor), electron transfer from the donor to the acceptor should occur more easily than the direct electron transfer in the D····A complex, because in the former the cooperative interaction of the three components should decrease the energy barrier of the electron transfer.

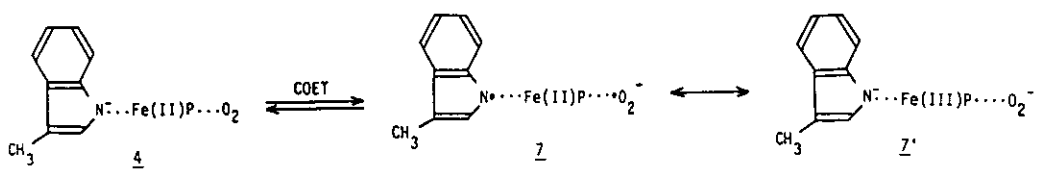

4 7 7'

This is an activation mechanism of molecular oxygen in the iron(II)porphyrin catalyzed oxygenation of skatole. We have termed this type of electron transfer (eq. 4) the cooperative (or concerted) electron transfer (COET).

$$D\cdots Fe(II)P\cdots A \xrightarrow{COET} D^{+}\bullet\cdots\cdots Fe(II)P\cdots\cdots A^{-} \qquad (4)$$

When the electron accepting power (electron affinity) of the accepter is less than that of molecular oxygen (EA: 0.43 eV), the electron donating power (ionization potential) of the donor must be larger than that of skatole anion for COET to occur. The MINDO/3 ionization potentials (I_p) for skatole and the skatole anion are shown in Table 3. This table indicates that by the deprotonation of the skatole NH, the HOMO (π) ionization potential becomes

Table 3 MINDO/3 Ionization Potential for Skatole and Skatole Anion

Species	Ionization Potential (eV)		
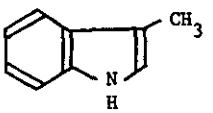	HOMO (π)	7.665	7.63 (obs*)
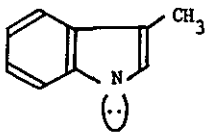	HOMO (π)	2.291	
	N-lone pair	3.101	

* H. Gusten et al., Z. Naturforsch., 319, 1051 (1976).

significantly smaller (7.665 eV → 2.291 eV). Also, the N-lone pair ionization potential (3.101 eV) of the skatole anion is close to the HOMO (π) ionization potential (2.291 eV). Therefore, the skatole anion is considered to be strong electron donor. From the ionization potentials of HOMO (π) and N-lone pair in non-interacted states, the generation of the π radical of the skatole anion should be easier than the generation of the σ radical (5). The observed exclusive formation of σ radical (5) in the ternary system might be caused by the effect of coordination with the iron(II) of the heme. The planar ligand, porphyrin, should make the axial coordination of both the donor and the acceptor possible and should also be useful in the

stabilization of this system. From the arguments mentioned above, the iron(II)porphyrin catalyzed oxygenation of skatole (and related compounds) most likely proceeds as shown in Scheme 1, which involves the π radical (6) intermediate. Process A is the equilibrium formation of the skatole anion-coordinated iron(II)porphyrin (8), which occurs with Fe(II) and solvent (B, π base) assistance. When the electron relay system 4 is formed by oxygen coordination, very rapid COET should take place to give the coordinated skatole σ radical and superoxide ion. Judging from the HOMO (π) and N-lone pair levels, this σ radical can interact with skatole anion to give the π radical (6). This π radical (6) should react easily with the superoxide ion of 9 to give the final product 10 via the most probable endo peroxide

Scheme 1

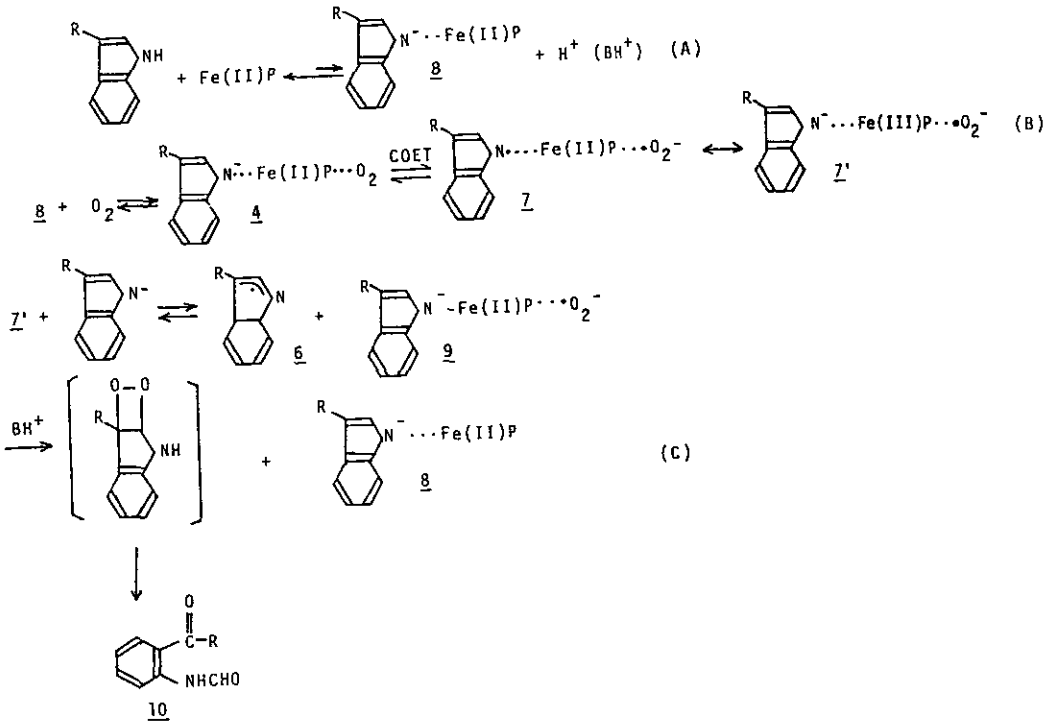

intermediate. The reproduced skatole anion-coordinated Fe(II)porphyrin (8) by process C is again reacted in Process B . The iron(II)porphyrin catalyzed oxygenation of skatole should proceed in this manner. This mechanism could be applicable to the TPO reaction. To establish the oxygen activation mechanism in TPO reaction, we have synthesized "indole-tail" porphyrin iron(III) complex (12) by the reaction of mono(o-aminophenyl)-triphenylporphyrin (10) with the mixed acid anhydride of 3-(2-indolyl)propionic acid with pivalic acid and the subsequent reaction with $FeCl_2$ (Scheme 2).

Scheme 2

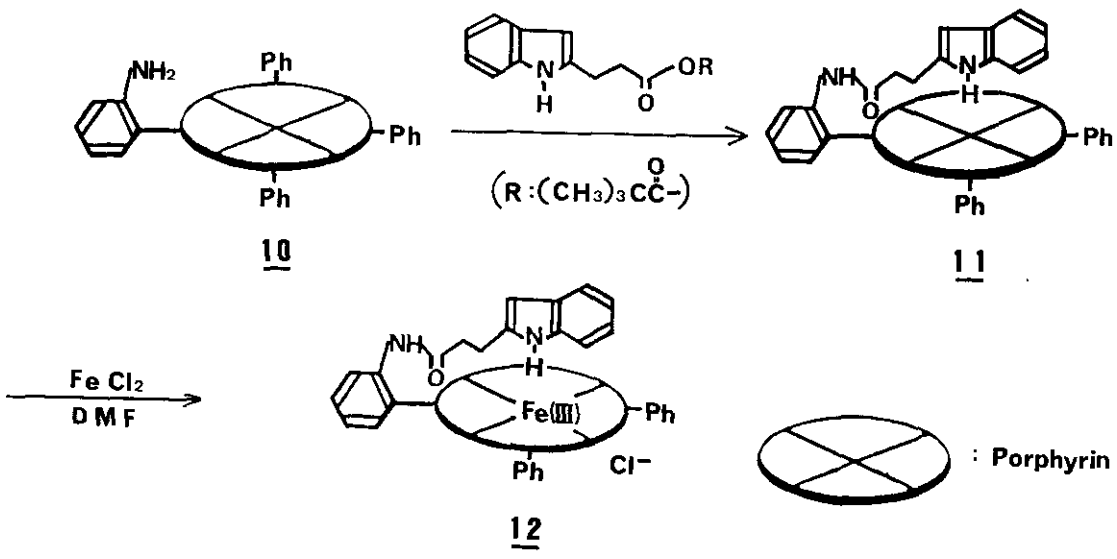

The indole-tail porphyrin-Fe(III) complex (12) ($\lambda_{max}^{benzene}$: 419, 509, 574, 656, 684 nm) is readily converted to the corresponding heme ($\lambda_{max}^{benzene}$: 426, 532, 562 nm) by hydrazine reduction. The CPK model of the complex 12 shows that its indole NH is situated just above the iron atom. Oxygenation of skatole (1.52 mmol) in benzene (5ml) using 12 (15.2 μmol) at room temperature (similar condition described above (eq. 2)) has very easily proceeded to afford foramidoacetophenone. Examination of the absorption spectra of 12 demonstrates that Fe(III) of 12 is rapidly and completely reduced to the Fe(II) state in benzene in the presence of pyridine or skatole. On the other hand, TPP Fe(III)Cl required the reducing agent ($n\text{-}Bu_4N^+BH_4^-$) for the complete conversion to heme state in the benzene-pyridine solution. As is seen Fig. 6, the indole-tail heme more efficiently catalized the oxygenation of skatole than does TPPFe(II). These data clearly indicate that intramolecularly bound indole (anion) is more useful as the COET-controlling ligand than intermolecularly bound indole (anion), and the indole-tail heme such as 12 is an excellent model for the active site of TPO.

Here I would like to point out how useful the heme (active site model for TPO) is for new organic synthesis. The highly selective and short step synthesis of α, ω-dicarboxylic acids has been desired so far because of its importance. Juding from the essential structural part (dotted line) of substrate for the TPO model reaction, imine derivative shown below might be a substrate for this reaction. From synthetic merits, we chose cycloalkanoneimine derivative (13) which has 3-substituted indole moiety. In the presence of hydroquinone monomethyl ether

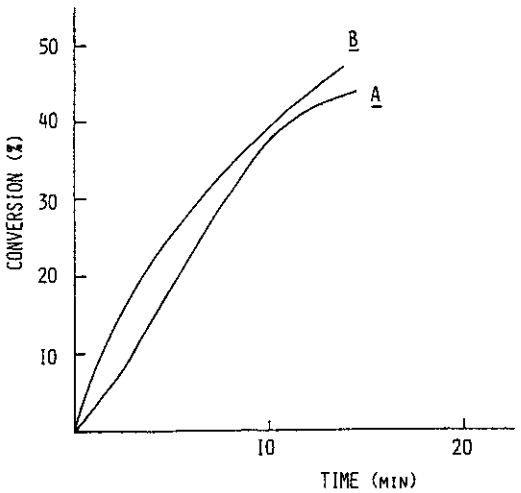

λ_{max}(Bz/Py) nm

A: TPPFe(III)Cl + n-$Bu_4\overset{+}{N}\bar{B}H_4$ (1:10) 425, 531

B: Indole-tail P Fe(III) 426, 532

Fig. 6 Oxygenation of skatole with indole-tail heme (Skatole 1.52mmol / Cat. 15.2 μmol / Benzene 5ml)

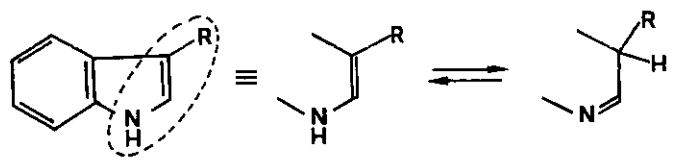

3-substituted indole β-substituted enamine β-substituted imine

(HQMME) as a reducing agent and catalytic amount of deuterohemine (DPFeCl), compound 13 was effectively oxygenated at room temperature to produce α, ω dicarboxylic acid derivative (14).

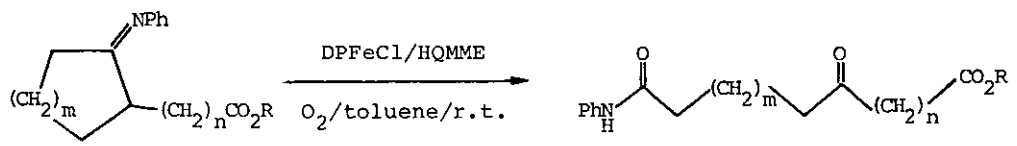

13 14

Some results are shown in Table 4. By changing m and/or n, we are able to synthesize various α, ω-dicarboxylic acid derivatives from 13. The carbonyl group of 14 can be reduced methylene or converted another functional group. Since the short path synthesis of α, ω -dicarboxylic acid is still unknown, this synthetic methodlogy is considered to have a useful application.

Table 4 Synthesis of α,ω-dicarboxylic acid derivatives from cycloalkanone imines

Substrate (13)	Product (14)	Isolated Yield (%)
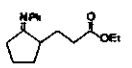	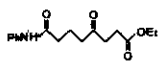	52
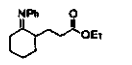	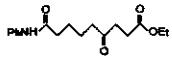	42
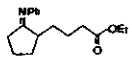	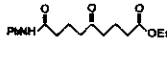	46
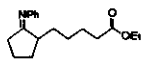	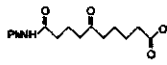	52
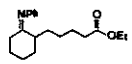	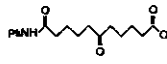	50

2. Monooxygenation Function of Porphyrin Oxovanadium Complex

Cytochrome P-450 is a typical monooxygenase whose oxygenation process is schematically shown in Scheme 3 where Fe, SH, LS and HS denote iron porphyrin, substrate, low spin state, and high spin state of Fe(III), respectively.

Scheme 3

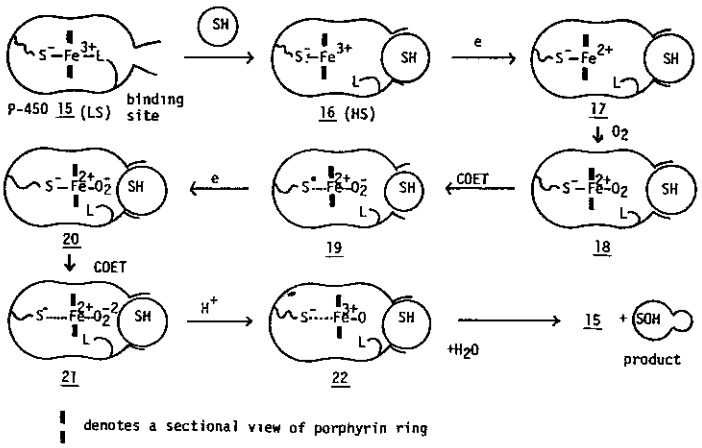

The key intermediate for P-450 reaction is considered to be the porphyrin $-Fe^{5+}= O^{2-}$ (22) which is too unstable to isolate because of easy breakdown of the $Fe^{5+}= O^{2-}$ bond of 22. In the first transition element series, the stability of transition metal (higher oxidation state) - oxygen bond ($M^{5+}= O^{2-}$) is expected to be a following order:

$$Ti^{5+} = O^{2-} > V^{5+} = O^{2-} > Cr^{5+} = O^{2-} > Mn^{5+} = O^{2-} > Fe^{5+} = O^{2-} > Co^{5+} = O^{2-}$$

In fact, porphyrin oxovanadium (vanadyl) or oxotitanium complex (porphyrin $M^{5+} = O^{2-}$, M: V or Ti) is known to be a very stable complex. Therefore, if the thermal or photochemical activation of the oxovanadium bond ($V^{5+} = O^{2-} \longrightarrow V^{4+}— O^{-}$ or $V^{3+}— O$) will be possible for the porphyrin oxovanadium complex, the (stoichiometric) monooxygenation will take place. Then if porphyrin $V^{5+}= O^{2-}$ complex will be reproduced from the resultant porphyrin V^{3+} complex and molecular oxygen, the P-450 type monooxygenation might be expected to occur in the presence of the catalytic amount of porphyrin $V^{5+}= O^{2-}$. As for the photochemical activation of $V^{5+}= O^{2-}$ bond, the charge transfer such as $V^{5+}= O^{2-} \xrightarrow{h\nu} V^{4+}— O^{-}$ is reported to occur by UV-irradiation ($\sim$ 330 nm) of vanadium oxide supported on silica (V_2O_5/SiO_2)[6], whose absorption appears at ca. 330 nm. Also it is reported[7] that although the UV-irradiation (340 nm) of V_2O_5/SiO_2 at room temperature is effective for oxydation of CO to CO_2, over pure vanadium oxide (V_2O_5) or vanadium oxide supported on alumina (V_2O_5/Al_2O_5) no photo-effects on the oxidation are observed.[7] Therefore it is not clear in the heterogeneous reactions whether photochemical activation of $V^{5+}= O^{2-}$ bond is easy or not. However it should be clear in the homogeneous reaction using porphyrin oxovanadium complex. From such considerations we synthesized tetraphenylporphyrin oxovanadium complex (TPP·$V^{5+}= O^{2-}$, 23) and octaethylporphyrin oxovanadium complex (OEP·$V^{5+}= O^{2-}$, 24) and tried to examine the epoxide formation from olefin and molecular oxygen using them (23, 24). The ultraviolet spectra of 23 (solution) show the appearance of a new band at 316 nm presumably due to the charge transfer band mentioned above.

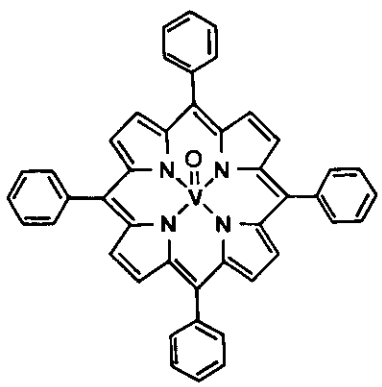

23

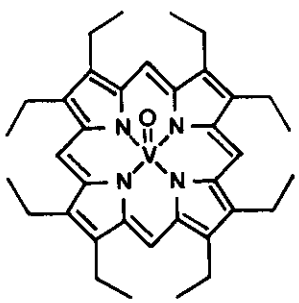

24

At first we examined the monooxygenation of cyclohexene as a substrate with molecular oxygen using 23 or 24 (10^{-4} mol ratio for cyclohexene) by thermal activation (50 ∿ 110 °C) and by photochemical activation (400 W Hg lamp irradiation). As a result we observed the formation of cyclohexene epoxide and cyclohexenol together with other oxidized products. The molar ratio of both products at low conversion of substrate (10 ∿ 20%) are shown in Table 5 together with other data. From this Table, the product ratio (A : B) for 23 seems to be close to the P-450 system. Then we applied our oxygenation using 23 to the direct epoxidation of olefins. Some of our results are shown below. As is seen there, although the conversion of the substrate is not high at present, the product selectivity is shown to be very high.

Table 5 Cyclohexene Oxygenation Catalyzed by P-450 and Model Systems

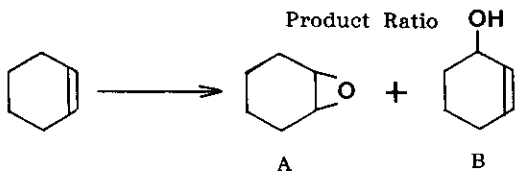

	A	B	A:B	
P-450/NADPH/O_2	0.92	1	0.92	Groves*
P-450/Cumene HP	12.2	13.8	0.88	Groves*
TPPFe(III)Cl/PhIO	55	15	3.7	Groves*
TPP(V=O)/O_2/ Δ	28	31	0.90	This work
TPP(V=O)/O_2/hν	17	19	0.89	This work
OEP(V=O)/O_2/ Δ	30	24	1.25	This work

* J. T. Groves et al., "Biomimetic Chemistry", D. Dolphin, etal., Eds.; (Advances in chemistry Series (91), Am. Chem. Soc.: Washignton, 1980, p. 277.

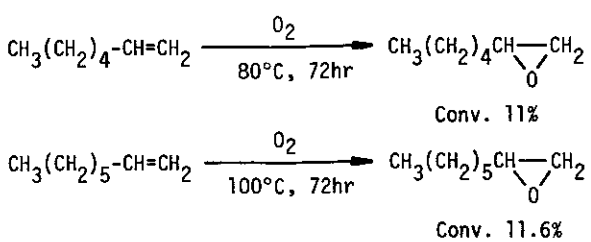

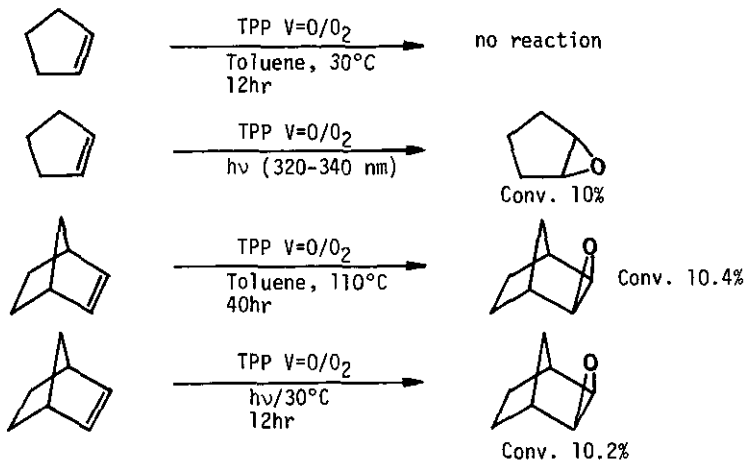

3. Catalytic Function of Porphyrin Cobalt Complex

One of the interesting functions of porphyrin cobalt complex is Vitamine B_{12}-mimetic function. For example, like Vitamine B_{12s} octaethylporphyrin Co(I) complex reacts with the following compounds to give Co(III)-C bond.[8]

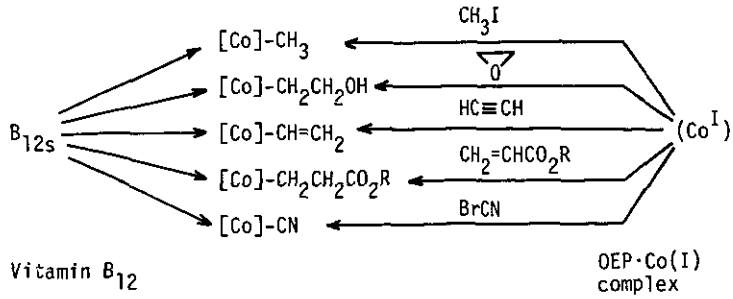

However these reactions are not due to the catalytic function of porphyrin cobalt complex. We examined the catalytic function of porphyrin cobalt complex for the conversion of quadricyclanes (26) to norbornadienes (25) where D and A are H or suitable substituents.

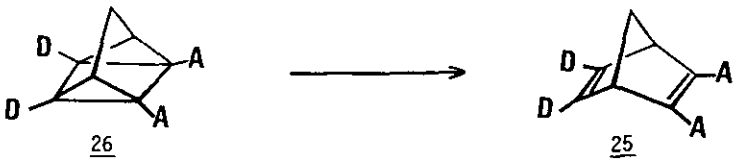

26 25 (5)

Consequently we found that although porphyrin Co(I) complex did not show the catalytic function for reaction 5, porphyrin Co(II) and Co(III) complexes catalyzed this reaction. Of both the Co(II) and Co(III) complexes the latter has high catalytic activity for conversion of quadricyclane to norbornadiene but the reaction become dirty. On the other hand, the former catalyst can control this reaction for the various quadricyclanes without any byproduct and the introduction of electron-withdrawing group into TPPCo(II) increases its catalytic activity. This is a very interesting finding because (1) the donor-acceptor norbornadiene (DA-norbornadiene 26 is extremely useful as new molecular energy storage system for sun light (eqs. 6 and 7) and

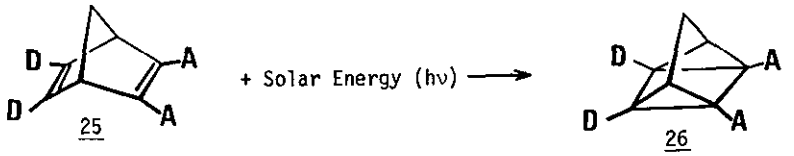

25 26 (6)

26 + Catalyst → 25 + heat (7)

(2) the so far reported transition metal complex catalysts have only poor catalytic activity for quadricyclane possessing high ionization potential. For practical application of the catalyst for this purpose, catalysts must be immobilized and repeatedly used with high activity. So, porphyrin cobalt(II) complex, for example, deuteroporphyrin IX Co(II) complex was immobilized using alumina functionalized with cationic polymer and its activity was examine using a bench-scale test plant made of Teflon (Fig. 7).

As shown in Fig. 7, the reactor is made 30 cm long and the two solution tanks are 5 ℓ in volume with two spare tanks (solution tanks). Feed is introduced into the reactor by means of a roller pump. The reactor is packed with the immobilized catalysts mentioned above (This is active part in Fig. 8). In the front and back sides of the catalyst layer glass beads are packed as an inert material. The reactor is thermaly insulated from its surroundings with asbestos. The twenty thermocouples are used to measure the temperature distribution in the

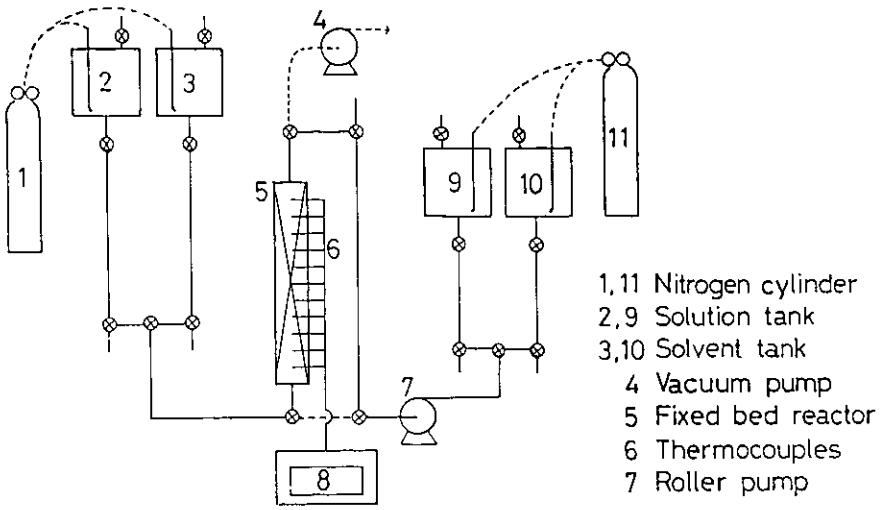

Fig. 7 Bench-scale test plant

reactor. A hybrid recorder is used to record the outputs of thermocouples. This bench-scale test plant showed an excellent performance in accordance with the design. That is, both conversions and temperature rises were close to equilibriums. The bench-scale test showed that the immobilized porphyrin cobalt (II) catalyst catalizes smoothly the cycloreversion process to generate heat (eq. 7), and is able to control the reaction 7 as shown in Fig. 8.

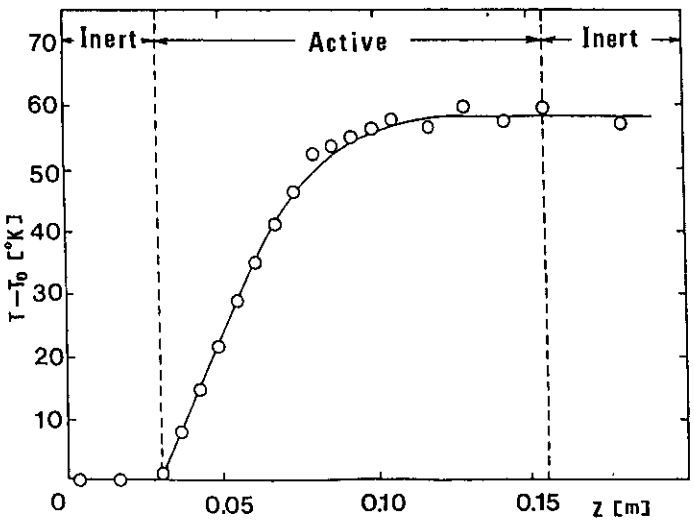

Fig. 8 Temperature distribution in the axial direction of the reactor

In Figure 8, $T-T_0$ is a difference between inner temperature (T) and entrance temperature (T_0) of the reactor, and Z is a distance from the entrance of reactor. As is seen in Fig. 8, as the quadricyclane solution (10%) passes through the catalytic layer, $T-T_0$ increases and finally reaches to the constant highest temerature. From this bench-scale test, porphyrin cobalt(II) complex is shown to be useful catalyst for the conversion of quadricyclanes to norbornadienes not only in the homogeneous system but also in heterogeneous system.

ACKNOWLEDGEMENT

I would like to express my appreciation to the following collaborators who have contributed to the work described above: Prof. H. Ogoshi, Dr. H. Sugimoto, Dr. K. Kawabe, Dr. S. Mitachi, Y. Fujita, Dr. K. Imai and Prof. I. Tyuma for the work of Section 1, Prof. H. Ogoshi, T. Koishi, K. Yamagata, and Y. Fujita for the work of Section 2, Dr. S. Miki, Dr. J. Setsune, Dr. E. Watanabe, T. Ono, Y. Asako and Dr. T. Maruyama for the work of Section 3. I wish also to thank the Ministry of Education, Science and Culture, Japan for financial support.

REFERENCES

1. K. Kawabe, K. Imaizumi, K. Imai, I. Tyuma, H. Ogoshi, T. Iwahara, and Z. Yoshida, J. Biochem., 1982, 92 1703.
2. Z. Yoshida, Pure and Applied Chemistry, 1981, 53, 293.
3. H. Ogoshi, H. Sugimoto, M. Miyake, and Z. Yoshida, Tetrahedron (Symposia-in-Print, "Bioorganic Studies on Receptor Sites") in press
4. Y. Ishimura, M. Nozaki, O. Hayaishi, M. Tamura, and I. Yamazaki, J. Biol. Chem., 1967, 242, 2574.
5. K. O. Hardman, E. H. Eylor, F. R. Gurd., J. Biol. Chem., 1966, 241, 432.
6. A. M. Gritskov, V. A. Shvets and V. B. Kazansky, Kinet. Katal., 1974, 15, 1257., Chem. Phys. Lett., 1975, 35, 511.
7. S. Yoshida, Y. Matsumura, S. Noda and T. Funabiki, J. Chem. Soc., Faraday Trans. I, 1981, 77, 2237.
8. H. Ogoshi, E. Watanabe, N. Koketsu, and Z. Yoshida, Bull. Chem. Soc. Jpn., 1976, 49, 2529.